

# PCCP

Physical Chemistry Chemical Physics

Accepted Manuscript

This article can be cited before page numbers have been issued, to do this please use: N. Shivran, S. P. Koiry, C. Majumder, A. K. Chauhan, D. K. Aswal, S. Chattopadhyay and S. Mula, *Phys. Chem. Chem. Phys.*, 2020, DOI: 10.1039/C9CP05918K.



This is an Accepted Manuscript, which has been through the Royal Society of Chemistry peer review process and has been accepted for publication.

Accepted Manuscripts are published online shortly after acceptance, before technical editing, formatting and proof reading. Using this free service, authors can make their results available to the community, in citable form, before we publish the edited article. We will replace this Accepted Manuscript with the edited and formatted Advance Article as soon as it is available.

You can find more information about Accepted Manuscripts in the [Information for Authors](#).

Please note that technical editing may introduce minor changes to the text and/or graphics, which may alter content. The journal's standard [Terms & Conditions](#) and the [Ethical guidelines](#) still apply. In no event shall the Royal Society of Chemistry be held responsible for any errors or omissions in this Accepted Manuscript or any consequences arising from the use of any information it contains.

## ARTICLE

## Tuning of electron tunneling: A case study using BODIPY molecular layers

Received 00th January 20xx,  
Accepted 00th January 20xx

Neelam Shivran,<sup>a</sup> Shankar P. Koiry,<sup>\*b,c</sup> Chiranjib Majumder,<sup>c,d</sup> Anil K. Chauhan,<sup>b,c</sup> Dinesh K. Aswal,<sup>c,e</sup> Subrata Chattopadhyay<sup>a</sup> and Soumyaditya Mula<sup>\*a,c</sup>

DOI: 10.1039/x0xx00000x

Redox active  $\pi$ -conjugated organic molecules have shown the potential to be used as electronic components such as diode and memory elements. Here we demonstrate that using simple surface chemistry, rectification characteristics can be tuned to reproducible negative differential resistance (NDR) with a very high peak-to-valley ratio (PVR) upto 1000 in 2,6-Diethyl-4,4-difluoro-1,3,5,7,8-pentamethyl-4-bora-3a,4a-diaza-s-indecene (BODIPY) grafted on Si. This change in properties is related to oxidation and reduction of BODIPY which results change in resonant to non-resonant tunneling of electrons under bias. This has been explained by the ab initio molecular-orbital theoretical calculations.

### Introduction

Two decades ago, the electrical characterization of organic molecules was started in a quest for tackling anticipated problems arising from the size reduction of Si-based transistors, which has been approaching fast to its physical limit [1]. However, the semiconductor industries find ways to invent new technologies and advance so much that many such technologies are waiting at our doorsteps, such as artificial intelligence and the Internet of Things (IoT) [2]. This advancement brings other challenges, for example, materials and devices required for IoT applications should be suitable for flexible substrates, extremely low powered, and capable of energy generation or scavenging. Thus, the arrival of newer technologies makes the studies of organic molecules for electronic applications even more relevant. Because electronic properties of organic molecules are studied only to make electronic devices faster, smarter, portable, flexible, and low powered.

Initially, molecules grafted to silicon wafers, known as hybrid nanoelectronics have been studied to develop various electronics components e.g. molecular diodes, molecular resonant tunnel diodes, molecular memory, molecular transistors etc. [3]. In view of the device applications in hybrid nanoelectronics, molecules grafted on Si should have reproducible electronics properties at room temperature.

The recent studies have almost identified which molecular structures would be useful for a particular electronic application. For example, the diode characteristics have been

shown in  $\sigma$ - $\pi$  systems which have high rectification ratio (RR) [3a, 3b, 4]. On the other hand, the  $\sigma$ - $\pi$ - $\sigma$  structures have shown the negative differential resistance (NDR) characteristic i.e. decreasing current with increasing voltage in particular voltage ranges with high peak to valley ratio (PVR) which has profound potential in the realization of logic devices and memory circuits [3a, 5].

For designing new molecules, it is prerequisite to get into the details of electron transports through such molecular structures. Since the size of the molecules is in the range of 0.7-3 nm, the charge transport through molecules and across molecule/electrode interfaces cannot be explained solely from classical semiconductor physics. At that nm range, electron transport is better understood by quantum mechanical tunneling. Thus the detailed understanding of charge transport is essential for developing next-generation molecular electronics.

Although, this research area is in developing state, different theories and experimental evidences have been proposed. The most widely acceptable explanation for rectification characteristics is resonant tunneling of electron through molecular energy levels of  $\pi$  moiety in  $\sigma$ - $\pi$  systems under forward bias. In reverse bias tunneling is non-resonant which results nonlinear current-voltage (J-V) characteristics. For NDR behaviours, two tunneling mechanisms are involved. During the current rise, the electron undergoes resonant tunneling through molecular energy levels of  $\pi$  moiety as explained for diode, and after further increase in voltage, the energy levels get shifted which causes non-resonant tunneling leading to decrease in current with increase in voltage. Thus, J-V characteristics of  $\sigma$ - $\pi$ - $\sigma$  structures show current peak in J-V measurements.

Recently, various organic molecules such as conjugated oligomers, redox-active-self-assembled monolayers, and hybrid materials also has shown NDR property [6-7]. To explain the observed NDR, several proposition have been given such as

<sup>a</sup> Bio-Organic Division, Bhabha Atomic Research Centre, Mumbai-400085, India.

<sup>b</sup> Technical Physics Division, Bhabha Atomic Research Centre, Mumbai-400085, India.

<sup>c</sup> Homi Bhabha National Institute, Anushakti Nagar, Mumbai 400094, India.

<sup>d</sup> Chemistry Division, Bhabha Atomic Research Centre, Mumbai-400085, India.

<sup>e</sup> National Physical Laboratory, New Delhi, 110012, India.

† E-mail: [spkoiry@barc.gov.in](mailto:spkoiry@barc.gov.in) (SPK) and [smula@barc.gov.in](mailto:smula@barc.gov.in) (SM)

Electronic Supplementary Information (ESI) available: [details of any supplementary information available should be included here]. See DOI: 10.1039/x0xx00000x

formation of radical anion or cation by charging and conformational changes [8]. Theoretical studies showed that the origin of NDR with hysteresis is associated with the polarization response, i.e., combined effects of charging and conformational change [9]. These theoretical studies predict that the molecules having redox properties and bias-induced conformational changes are potential candidate for NDR effect with hysteresis. It could be envisioned that the bias induced conformational changes are difficult to accommodate in a chemical bonded molecular layer. However, the change of conformation would be easier to apprehend for the molecular layers which are formed by weak physical interactions. This strategy is explored here using bilayer of BODIPY (4,4-Difluoro-4-bora-3a,4a-diaza-s-indacene) [10] molecules in which one layer has  $\sigma$ - $\pi$  structures grafted on Si and other layer (only  $\pi$  moiety), formed by van der Waals force [11a].

The BODIPY class of compounds have robust reversible redox properties [12]. These properties can be tuned by varying different substituent on the dye chromophore to use in OLEDs, solar cell etc. [13]. This reversible redox property of BODIPY dyes and their robust stability under ambient conditions could be very useful for their use in hybrid nanoelectronics which still remains unprecedented. In this report, we discussed rectification property of a tailor made BODIPY dye ( $\sigma$ - $\pi$  moiety) grafted on Si and how this property can be tuned to NDR property by forming bi-layer with another BODIPY molecule (only  $\pi$  moiety).

## Experimental

### General methods

For synthesis of BODIPY-C5, the chemicals and spectroscopic grade solvents were purchased from Aldrich, Merck or Sigma and were used without any further purification. PM567 was purchased from Aldrich and was used without any further purification. The Fourier transform infrared spectra (FTIR) were recorded with a Nicolet 430 FT-IR spectrophotometer. The  $^1\text{H}$  NMR and  $^{13}\text{C}$  NMR spectra were recorded with a Bruker 200 FT-spectrometer in  $\text{CDCl}_3$ . The mass spectra (70 eV) were recorded with a MD-80 Fission instrument. The surface morphology of mono/bilayer was characterized by AFM imaging (Multiview 4000, Nanonics) and molecular mass by SIMS (BARC make, Kore's Technology software). The current voltage characteristics were recorded in a dark box using a potentiostat/galvanostat system (model: Autolab PGSTAT 30). The thickness of the films was measured using an ellipsometer (Sentech: model SE400adv); For measurement, a Si/organic layer/Air model was designed. Before deposition of monolayers on Si, we measured  $n$  and  $k$  values for the substrate. After organic layer deposition, we used measured  $n$ ,  $k$  value of the substrate and assumed  $n = 1.5$  and  $k = 0$  for organic. With these input values, model was fitted to obtained thickness of the organic layer.

### Synthetic procedures

**Synthesis of 4-(4'-penentenloxy)benzaldehyde (2).** A mixture of 4-hydroxybenzaldehyde (4.0 g, 32.7 mmol), 5-bromo-1-pentene (4.7 mL, 39.3 mmol),  $\text{K}_2\text{CO}_3$  (5.52 g, 40 mmol) and  $\text{Bu}_4\text{NI}$  (10 mol%) in acetone (100 mL) was refluxed. After completion of the reaction (cf. TLC  $\sim$  16 h) the mixture was filtered, concentrated in vacuum, the residue taken in  $\text{Et}_2\text{O}$  (40 mL) and washed with  $\text{H}_2\text{O}$  ( $2 \times 10$  mL) and brine ( $1 \times 20$  mL), dried and concentrated in *vacuo*. The residue was purified by column chromatography (silica gel, 5%  $\text{EtOAc}$ /hexane) to give pure 2 (5.7 g, 91%) as viscous liquid. IR: 3019, 1687  $\text{cm}^{-1}$ ;  $^1\text{H}$  NMR (200 MHz,  $\text{CDCl}_3$ , 25  $^\circ\text{C}$ , TMS):  $\delta$  1.28-1.42 (m, 2H), 2.32 (t,  $J = 6.8$  Hz, 2H), 4.01 (t,  $J = 6.2$  Hz, 2H), 6.97 (d,  $J = 9.5$  Hz, 2H), 7.80 (d,  $J = 9.5$  Hz, 2H), 9.85 (s, 1H);  $^{13}\text{C}\{^1\text{H}\}$  NMR (50 MHz,  $\text{CDCl}_3$ , 25  $^\circ\text{C}$ , TMS):  $\delta$  13.6, 22.2, 25.3, 28.7, 31.2, 68.1, 114.4, 129.6, 131.5, 163.9, 190.1; Anal. Calcd. for  $\text{C}_{12}\text{H}_{14}\text{O}_2$ : C, 75.76; H, 7.42%. Found: C, 75.44; H, 7.16%.

**Synthesis of 2,6-Diethyl-4,4-difluoro-1,3,5,7-tetramethyl-8-(4'-(4''-penteneoxyphenyl)-4-bora-3a,4a-diaza-s-indecene (BODIPY-C5).** A mixture of 2,4-dimethyl-3-ethyl-1H-pyrrole (1) (1.00 g, 8.13 mmol), 4-(4'-penentenloxy)benzaldehyde (2) (0.70 g, 3.7 mmol) and TFA (1 drop) in  $\text{CH}_2\text{Cl}_2$  (30 mL) was stirred at 25  $^\circ\text{C}$  for 12 h. DDQ (0.84 g, 3.7 mmol) was added to the resulting deep color solution and stirring continued for 4 h. The mixture was treated with  $\text{Et}_3\text{N}$  (3.1 mL) and stirred for 10 min. Finally,  $\text{BF}_3 \cdot \text{Et}_2\text{O}$  (2.8 mL, 22.2 mmol) was added into the mixture and the solution stirred at room temperature for 12 h. The resulting dark mixture was washed with aqueous saturated  $\text{NaHCO}_3$  (50 mL),  $\text{H}_2\text{O}$  (50 mL) and brine (50 mL) and dried. Removal of solvent in vacuum followed by column chromatography of the residue (silica gel, hexane- $\text{EtOAc}$ ) furnished BODIPY-C5 (0.24 g, 13.7%), which was recrystallized from  $\text{CH}_2\text{Cl}_2$ /cyclohexane to afford red square shaped crystals. Mp: 177-178  $^\circ\text{C}$ ; IR: 2964, 2880, 1608, 1643  $\text{cm}^{-1}$ ;  $^1\text{H}$  NMR (200 MHz,  $\text{CDCl}_3$ , 25  $^\circ\text{C}$ , TMS):  $\delta$  0.98 (t,  $J = 7.6$  Hz, 6H), 1.34 (s, 6H), 1.93 (t,  $J = 7.7$  Hz, 2H), 2.16-2.36 (m, 6H), 2.53 (s, 6H), 4.03 (t,  $J = 6.5$  Hz, 2H), 5.00-5.12 (m, 2H), 5.89-5.99 (m, 1H), 7.01 (d,  $J = 6.7$ , 2H), 7.13 (d,  $J = 6.7$ , 2H);  $^{13}\text{C}\{^1\text{H}\}$  NMR (50 MHz,  $\text{CDCl}_3$ , 25  $^\circ\text{C}$ , TMS):  $\delta$  11.7, 12.4, 14.5, 17.0, 28.3, 30.0, 67.2, 114.9, 115.2, 127.6, 129.3, 131.1, 132.5, 137.5, 138.4, 140.3, 153.3, 159.4; EI-MS ( $m/z$ ): 464.0 ( $\text{M}^+$ ); Anal. Calcd. For  $\text{C}_{28}\text{H}_{35}\text{BF}_2\text{N}_2\text{O}$ : C, 72.42; H, 7.60; N, 6.03%. Found: C, 72.05; H, 7.91; N, 6.28%.

### Measurement of current-voltage characteristics

To measure current-voltage ( $J$ - $V$ ) characteristics, a metal/monolayer or bilayer/Si( $n^{++}$ ) structure was completed by using a very small drop of liquid mercury as a counter electrode. The  $J$ - $V$ 's were recorded at room temperature by scanning the bias in the sequence  $-1.8 \text{ V} \rightarrow 0 \text{ V} \rightarrow +1.8 \text{ V} \rightarrow 0 \text{ V} \rightarrow -1.8 \text{ V}$  at a scan speed was 5 mV/s in a dark box using HP4140 (pA meter-dc voltage source). Room temperature  $J$ - $V$  characteristic recorded for un-deposited Si surface is shown in Figure 1.

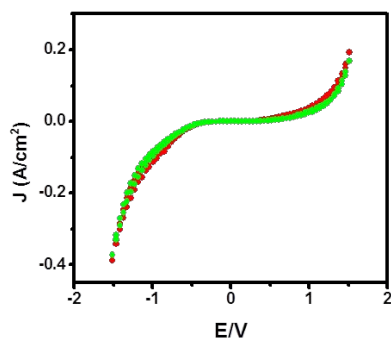


**Figure 1.** Room temperature J-V characteristic recorded for un-deposited Si surface by scanning the bias in the sequence  $-1.5\text{ V} \rightarrow 0\text{ V} \rightarrow +1.5\text{ V} \rightarrow 0\text{ V} \rightarrow -1.5\text{ V}$  at a scan speed of  $5\text{ mV/s}$ .

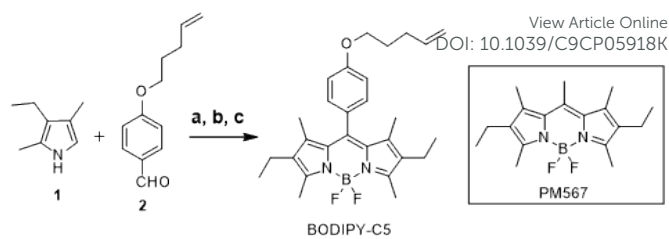
### Theoretical computation

The highest occupied molecular orbital (HOMO) and lowest unoccupied molecular orbital (LUMO) energies for neutral, and at different oxidation state of BODIPY-C5 and PM567: BODIPY-C5 molecules respectively were calculated theoretically. The geometries and total energies of molecules were optimized under the density functional theory using the linear combination of atomic orbital (LCAO) approach using General Atomic and Molecular Electronic Structure System (GAMESS). A standard 6-31G+(d,p) basis set was employed for this purpose. The exchange correlation energy was calculated using B3LYP functional. This functional uses part of Hartree-Fock exchange and Becke's exchange functional, and the Lee-Yang-Parr correlation functional. For the computation, we have used PC and two supercomputers, namely, Ameya and Ajeya. Ameya is 128-processor ANUPUM supercomputer built on 64 dual Xeon servers (2.4 GHz) as compute node, interconnected by a high-speed (300 MBps) communication network. The 512-processors ANUPAM-ameya supercomputer is built using 256 dual Xeon servers as a compute node. Each server is based on dual Xeon, 3.6 GHz processors. The inter-communication network is Gigabit Ethernet with a node-to-node communication speed of 1 Gbps. The performance of ANUPAM-ameya is 1.73 Teraflops. The open source Linux operating system is used on each parallel processing node in these two supercomputers.

## Results and discussion

### Design and synthesis

2,6-Diethyl-4,4-difluoro-1,3,5,7-tetramethyl-8-(4'-(4"-pentenoxyphenyl)-4-bora-3a,4a-diaza-s-indecene (BODIPY-C5) (Scheme 1) was designed first in order to graft it on  $\text{Si}(n^{++})$  surface. BODIPY-C5 has a C-5 alkyl chain terminated with C=C group, which is essential for its electrografting to  $\text{Si}(n^{++})$  [3a, 4]. For the bi-layer formation, another BODIPY dye, PM567 (Scheme 1) was chosen because of its planar structure which can easily intercalate into the self-assembled mono layer of BODIPY-C5.

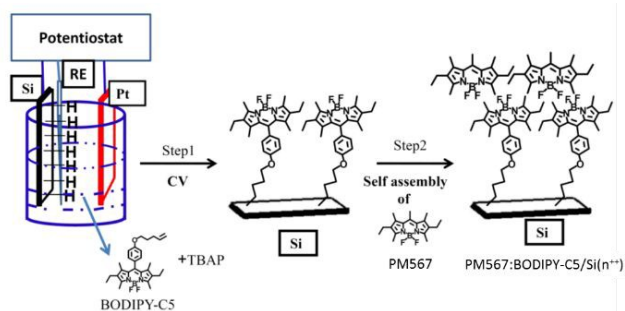


**Scheme 1.** Synthesis of BODIPY-C5 and chemical structure of PM567. a) TFA,  $\text{CH}_2\text{Cl}_2$ ,  $25\text{ }^\circ\text{C}$ , 4 h; b) DDQ,  $25\text{ }^\circ\text{C}$ , 4 h; c) TEA,  $\text{BF}_3 \cdot \text{Et}_2\text{O}$ ,  $25\text{ }^\circ\text{C}$ , 12 h.

At first, 4-(4'-pentenoxy)benzaldehyde (2) was synthesized by base-catalyzed alkylation of 4-hydroxybenzaldehyde with 5-bromo-1-pentene. Then, TFA-catalyzed condensation of 2 with kryptopyrrole (1) furnished the dipyrromethane which was subjected to oxidation with DDQ, followed by complexation with  $\text{BF}_3$  in the presence of  $\text{Et}_3\text{N}$  as the base to afford BODIPY-C5 (Scheme 1). The structure of BODIPY-C5 was confirmed by analysing its NMR spectra in  $\text{CDCl}_3$ . For example,  $^1\text{H}$  NMR spectrum (Figure S3(a)) showed two doublets for aromatic protons with expected two protons integration for each signal. The vinyl group of the pentenoxy lateral chain resonated as two different multiplets at 5.95 (one proton) and 5.05 ppm (two protons). Diagnostic triplet for the pentenoxy methylene group appeared at 4.03 ppm. Four benzylic methyl groups attached to the BODIPY core resonated as two singlets at 2.53 and 1.34 ppm with the expected six protons integration for each signal. Another diagnostic triplet for the terminal methyl groups of the ethyl chains of the BODIPY core appeared at 0.98 ppm with six protons integration. The carbon spectrum showed six signals for the alkyl atoms, expected 11 signals for aromatic and alkene atoms, and one diagnostic signal for pentenoxy group (Figure S3(b)).

### Preparation of the $\text{Si}(n^{++})$ -BODIPYs assemblies

BODIPY bilayer on H-terminated  $\text{Si}(n^{++})$  substrates was deposited in two steps (Scheme 2) (see supplementary information for details). In the first step, monolayer of BODIPY-C5 was electrografted to H-terminated  $\text{Si}(n^{++})$  (Figure S2). The electrografting mechanism of BODIPY-C5 to H- $\text{Si}(n^{++})$  is based on formation of Si-radicals on application of negative potential, which reacts with C=C group of the molecules to form Si-C bond (Figure S1) [14]. Electrografted BODIPY-C5/ $\text{Si}(n^{++})$  was sonicated in dichloromethane, acetone and methanol for 10 min to remove any physisorbed molecules. In the second step, PM567 monolayer was self-assembled on electrografted BODIPY-C5/ $\text{Si}(n^{++})$  by dipping it into dichloromethane solution of PM567 for 24 h in inert atmosphere. It is proposed that PM567 through its F atoms form hydrogen bonds, i.e., B-F...H-C with surface terminating  $\text{CH}_3$  groups of BODIPY-C5/ $\text{Si}(n^{++})$  monolayer (Scheme 2) [11a].



**Scheme 2.** Pictorial representation of two steps deposition process of BODIPY on Si(n<sup>++</sup>). Step 1: Electrografting of BODIPY-C5 monolayer on H-Si(n<sup>++</sup>); Step 2: formation of bilayer by self-assembly of PM567 onto BODIPY-C5/Si(n<sup>++</sup>).

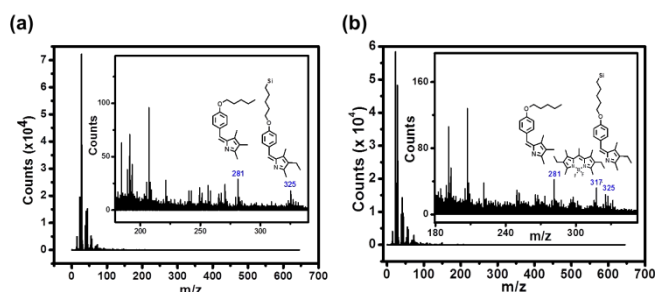
Hydrogen bonding ability of the covalently bound fluorine atoms is questioned previously [11b]. However, distinct C–H...F hydrogen bond interactions were reported to stabilize the layered crystal structure of fluoroaromatics [11c], and to form robust supramolecular assemblies of organic molecules [11d] including BODIPYs [11a]. In the present case also, C–H...F hydrogen bond interactions help to form bilayer BODIPY.

In bilayer, as the surface is not terminated by F atoms, possibility of multilayer formation does not exist. This in fact has been experimentally confirmed by dipping the BODIPY-C5 monolayer in PM567 solution for several days, as well as by increasing its concentration. In all these experiments, no increase in the film thickness was found.

### Characterization of modified surfaces

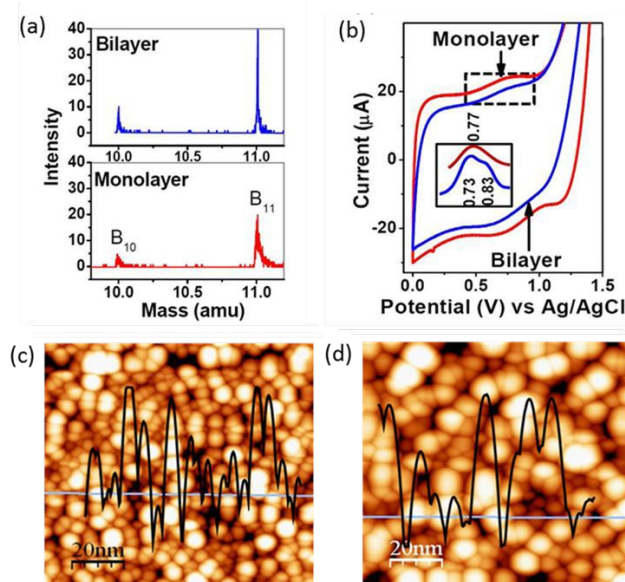
The electrografting of the BODIPY-C5 monolayer on Si(n<sup>++</sup>) and the formation of PM567:BODIPY-C5/Si(n<sup>++</sup>) bilayer was experimentally confirmed by several techniques, such as secondary ion mass spectrometry (SIMS), electrochemical characterization, ellipsometry and atomic force microscopy (AFM).

The SIMS data of the monolayer of BODIPY-C5 showed peaks at *m/z* 325 and 281 amu due to the BODIPY fragments (Figure 2(a)). Interestingly, the SIMS data of the bilayer PM567:BODIPY-C5/Si(n<sup>++</sup>) showed an additional mass peak at *m/z* 317 amu, accounting for the [M-1]<sup>+</sup> peak for PM567 along



**Figure 2.** TOF-SIMS of positive secondary ions desorbed from monolayer and bilayer by mono-isotopic <sup>69</sup>Ga projectile. (a) BODIPY-C5/Si(n<sup>++</sup>) monolayer; (b) PM567:BODIPY-C5/Si(n<sup>++</sup>) bilayer. (insets: enlarged plots.)

with the peaks due to the BODIPY fragments (Figure 2(b)). Also, the SIMS data shown in Figure 3(a) shows fragmented boron species B<sub>10</sub> and B<sub>11</sub> of BODIPY and, as expected, the number of boron atoms in bilayer is nearly double than that of monolayer. Thus, the SIMS data confirmed deposition of their respective layers on the Si wafers.



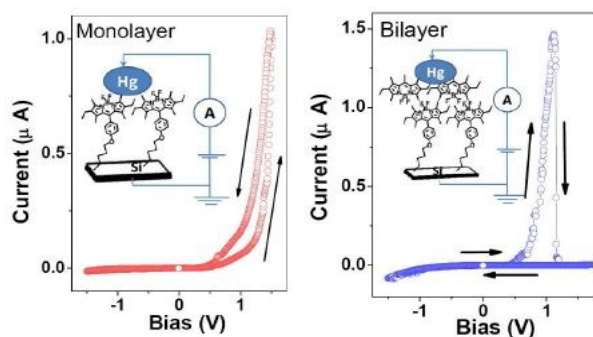
**Figure 3.** (a) Time-of-flight secondary ion mass spectra of positive secondary ions desorbed from monolayer and bilayer by mono-isotopic <sup>69</sup>Ga projectile. (b) Typical fast scan (100V/s) CVs recorded using 0.1M TBAP in dichloromethane with BODIPY monolayer or bilayer as working electrodes. Inset shows the magnified version of the oxidation peaks after subtraction of the background. (c) and (d) The noncontact atomic force microscope images recorded for monolayer and bilayer, respectively.

Figure 3(b) shows the fast scan (100 V/s) cyclic voltammograms (CVs) recorded for BODIPY-C5/Si(n<sup>++</sup>) or bilayer PM567:BODIPY-C5/Si(n<sup>++</sup>) as working electrode (surface area = 0.025 cm<sup>2</sup>) and 0.1 M TBAP as electrolyte with a Pt counter-electrode and a Ag/AgCl reference electrode. As shown in the inset of Figure 3(b), monolayer exhibits a single peak at 0.77 V, indicating only one oxidation for BODIPY-C5 molecules. Whereas, bilayer exhibits two closely spaced peaks at 0.73 V and 0.83 V, indicating that bilayer undergoes a double oxidation.

Both mono- and bilayers exhibit granular surface morphology with an average grain size of 8 and 14 nm, respectively (Figure 3(c) and 3(d)). The thickness of the mono- and multilayer, as measured by ellipsometry, was found to be respectively, 1.1±0.2 and 1.9±0.2 nm, which are in agreement with corresponding theoretical lengths of BODIPY-C5 (1.2 nm) and PM567:BODIPY-C5 (1.86 nm) molecules.

### J-V characteristics

As shown in Figure 4, the J-V characteristics of monolayer and bilayer are remarkably different. The monolayer exhibits a rectification behavior, which is in accordance with that predicted for  $\sigma$ - $\pi$  molecular rectifiers [3a, 3b]. The rectification ratio (RR) i.e. ratio of current at -1.5 V (in absolute value) and the current at 1.5 V ( $RR = |J_{-1.5V}| / |J_{1.5V}|$ ) was  $\sim 64$ . The RR value measured for 50 samples are varied in the range of 40-70, and more than 90% samples showed rectification behaviours. It is important to mention that the J-Vs of these diodes exhibit hysteresis which may be due to formation of electric dipole under high-applied electric field. RR decreases with repeated measurements but the initial value of RR was restored by keeping the structure is at zero voltage for about 10 min. Similar observation was also reported previously [15]. On the other hand, bilayer exhibited a strong NDR effect in concomitant with a pronounced hysteresis. The room temperature PVR values measured for 80 samples. Around 50% of samples show PVR values between 670 and 1000, which are the very high values as compared to reported values till date for the molecules covalently grafted on Si [3d, 5]. Among the rest, the values are lying between 100-600 ( $\sim 30\%$ ) and 50-100 ( $\sim 20\%$ ). However, during the experiment, we also encountered no results in a few samples, which are because of the device got short-circuited due to improper sample preparation. It may be noted that NDR is obtained only in the first bias scan and in the subsequent bias scans NDR disappears as the current remains low. The NDR effect reappears after the electrodes are short-circuited which is discussed *vide infra*.



**Figure 4.** (a) Room temperature J-V characteristic recorded for BODIPY monolayer and bilayer by scanning the bias in the sequence  $-1.8\text{ V} \rightarrow 0\text{ V} \rightarrow +1.8\text{ V} \rightarrow 0\text{ V} \rightarrow -1.8\text{ V}$  at a scan speed was 5 mV/s. Inset shows the schematic of the structures employed for the measurements.

### Theoretical explanation

One way to visualize the cause of such J-V characteristics is to draw an energy levels diagram with respect to vacuum, and to depict electron transport across the energy levels under applied electric field. For this purpose, the highest occupied molecular orbital (HOMO) and lowest unoccupied molecular orbital (LUMO) energies of BODIPY-C5 and PM567:BODIPY-C5 molecules were calculated using molecular orbital theory

method, as implemented in GAMESS software to explain the observed rectification and NDR behaviors of monolayer and bilayers, respectively [16]. Optimization of the geometries and total energies of molecules were done by the density functional theory calculations using the linear combination of atomic orbital (LCAO) approach with a standard 6-31G+(d,p) basis set. The exchange correlation energy was calculated using B3LYP functional, which consists of Hartree-Fock exchange, Becke's exchange and Lee-Yang-Parr correlation functional [16]. Theoretically, it was found that BODIPY-C5 undergoes for a single oxidation; while PM567:BODIPY-C5 undergoes for double oxidation. This inference is in agreement with the experimental results presented in the Figure 3(b). Bilayer undergoing double oxidation is expected as it has two BODIPY layers. Theoretically calculated spatial orientation of HOMO's of neutral and, after I<sup>st</sup> and II<sup>nd</sup> oxidations of PM567:BODIPY-C5 are shown in Figure 5(a). It is seen that in the neutral state the HOMO lies on the PM567:BODIPY-C5 moiety and after I<sup>st</sup> oxidation though it more or less remains on PM567:BODIPY-C5 moiety but with a slight conformational change. However, after II<sup>nd</sup> oxidation, there is huge conformational change as the HOMO largely shifts to the alkyl-chain and this could be attributed to slippage or rotation of PM567:BODIPY-C5 interface, which is weakly bonded though B-F...H-C type hydrogen bonds.

One of the best ways to understand the electron transport, is to draw the schematic energy level diagrams of the Hg/PM567:BODIPY-C5/Si(n<sup>++</sup>) structure and to correlate with observed J-V characteristics (Figure 5(b)). To draw the schematic, we use theoretically calculated HOMO (-5.25, 5.26 eV) and LUMO (-2.01, -2.07 eV) energy levels of neutral PM567:BODIPY-C5, and the standard Fermi levels of Hg and Si. For neutral state, doubly degenerate and singly occupied HOMO levels indicate the possibility of double oxidation of PM567:BODIPY-C5, which is in agreement with experimental data presented in Figure. 1 (a). As shown in the Figure 5 (b), the

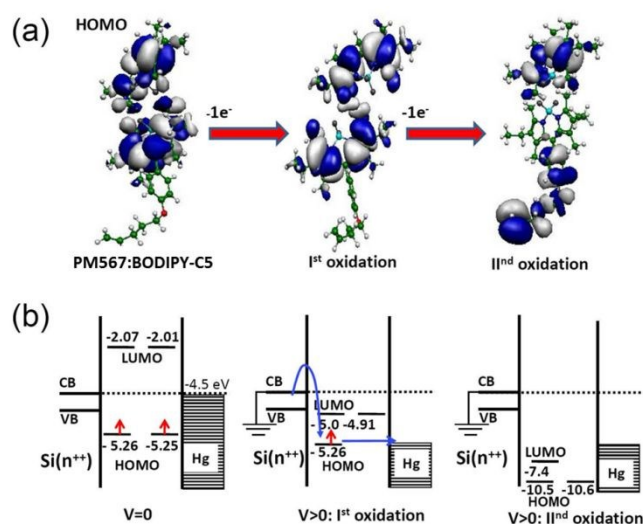


**Figure 5.** (a) Theoretically calculated geometrical orientation of HOMO of PM567:BODIPY-C5 under different oxidation states. (b) Schematic representation of the energy level diagrams for Hg/PM567:BODIPY-C5/Si(n<sup>++</sup>) device at different applied bias.

degenerate HOMO and LUMO levels of PM567:BODIPY-C5 are off-resonance with the Fermi level of the Hg electrode at zero bias i.e.  $V=0$ . For an applied positive bias ( $V>0$ ), a rise in current in the J-V (see Figure 4) is attributed to non-resonant tunneling. A sharp rise in current above  $> 0.8V$  as per the J-V curve (Figure 5 (b)) would be attributed to the alignment of the Fermi level of Hg with HOMO energy levels. The alignment results in resonant tunneling through HOMO. Even if the bilayer undergoes I<sup>st</sup> oxidation, the current keeps rising sharply because the oxidation does not bring any significant changes in the conformation (Figure 5(a)). Moreover, the LUMOs of oxidized molecules come under the applied potential window and consequently would also take part in electron transport enhancing current further (Figure 5(b)). However, at further higher bias, the current drops sharply, which could explain from II<sup>nd</sup> oxidation of the bilayer. The doubly oxidized bilayer undergoes a large conformational change, see Figure 5(a). Consequently, the HOMO and LUMO levels are shifted and become off-resonance to the Fermi level of Hg. As a result, the current now can pass only through the direct tunneling process, which manifests as the NDR effect in J-V measurements. We also observed that the current always remains low in the subsequent J-V cycles. However, if the electrodes are short-circuited, the neutral state of the PM567:BODIPY-C5 is regained, and hence, the NDR effect reappears. Thus it is inferred that the conformational changes achieved after II<sup>nd</sup> oxidation are quite stable.

On the other hand, for negative bias on Hg electrode i.e.  $V<0$ , the current remains low as a very high bias is required to obtain a resonance between the Hg Fermi level and LUMO of the molecule. Moreover, the molecule does not undergo for any reduction, and therefore, no additional feature other than non-resonant tunneling current, appears in the negative bias. In the case of monolayer i.e. Hg/BODIPY-C5/Si( $n^{++}$ ) structure, observed rectification behavior is similar to those of  $\sigma$ - $\pi$  molecular diodes, which arises because of resonant tunneling through the HOMO of the  $\pi$  group [17]. Since BODIPY-C5 molecule does not undergo II<sup>nd</sup> oxidation and major conformational changes do not occur, therefore no NDR effect is observed in this case.

## Conclusions

In conclusion, we have demonstrated the strategy to tune the electrical behavior of BODIPY dye grafted on Si. The tailor-made BODIPY-C5 moiety grafted on Si showed rectification property while BODIPY bilayers grafted on Si showed room temperature NDR effect with PVR upto 1000. Our studies show that rectification characteristics are due to resonant tunneling. However, the NDR behaviour is associated with bias induced conformational changes of the bilayer molecules by which the resonant tunneling is changed to non-resonant tunneling. These results are important for the development of resonant tunnel diodes for molecules-on-Si hybrid nanoelectronics and single molecular based futuristic electronics.

## Conflicts of interest

There are no conflicts to declare.

## Acknowledgements

We thank Dr. K. G. Bhusan for conducting the SIMS measurements.

## Notes and references

- 1 a) M. -Y. Li, S. -K. Su, H. -S. P. Wong and L. -J. Li, *Nature*, 2019, **567**, 169-170; b) M. C. Petty in *Molecular Electronics: From Principles to Practice*, Wiley, 2008; c) P. T. Mathew and F. Fang, *Engineering*, 2018, **4**, 760-771.
- 2 <https://eps.ieee.org/images/files/Roadmap/SIA-SRC-Vision-Report-3.30.17.pdf>
- 3 a) D. K. Aswal, S. Lenfant, D. Guerin, J. V. Yakhmi and D. Vuillaume, *Anal. Chim. Acta.*, 2006, **568**, 84-108; b) A. Salomon, D. Cahen, S. Lindsay, J. Tomfohr, V. B. Engelkes and C. D. Frisbie, *Adv. Mater.*, 2003, **15**, 1881-1890; c) M. Laurans, K. Dalla Francesca, F. Volatron, G. Izzet, D. Guerin, D. Vuillaume, S. Lenfant and A. Proust, *Nanoscale*, 2018, **10**, 17156-17165; d) T. Rakshit, G. -C. Liang, A. W. Ghosh and S. Datta, *Nano Lett.*, 2004, **4**, 1803-1807.
- 4 K. Garg, C. Majumder, S. K. Gupta, D. K. Aswal, S. K. Nayak and S. Chattopadhyay, *Chem. Sci.*, 2016, **7**, 1548-1557.
- 5 K. Garg, C. Majumder, S. K. Gupta, D. K. Aswal, S. K. Nayak and S. Chattopadhyay, *RSC Adv.*, 2015, **5**, 50234-50244.
- 6 a) Q. Tang, H. K. Moon, Y. Lee, S. M. Yoon, H. J. Song, H. Lim and H. C. Choi, *J. Am. Chem. Soc.*, 2007, **129**, 11018-11019; b) R. A. Wassel, G. M. Credo, R. R. Fuierer, D. L. Feldheim and C. B. Gorman, *J. Am. Chem. Soc.*, 2004, **126**, 295-300; c) R. Khurana, J. Mohanty, N. Padma, N. Barooah and A. C. Bhasikuttan, *Chem. Eur. J.*, 2019, 10.1002/chem.201902641; d) P. Chal, A. Shit, D. Levy, S. Das, S. Mondal and A. K. Nandi, *Colloids Surf. A: Physicochemical and Engineering Aspects*, 2019, **577**, 480-492.
- 7 a) J. Chen, M. A. Reed, A. M. Rawlett and J. M. Tour, *Science*, 1999, **286**, 1550; b) Z. J. Donhauser, B. A. Mantooth, K. F. Kelly, L. A. Bumm, J. D. Monnell, J. J. Stapleton, D. W. Price, A. M. Rawlett, D. L. Allara, J. M. Tour and P. S. Weiss, *Science*, 2001, **292**, 2303; c) J. L. Pitters and R. A. Wolkow, *Nano Lett.*, 2006, **6**, 390-397; d) N. P. Guisinger, M. E. Greene, R. Basu, A. S. Baluch and M. C. Hersam, *Nano Lett.*, 2004, **4**, 55-59; e) Y. Selzer, A. Salomon, J. Ghabboun and D. Cahen, *Angew. Chem. Int. Ed.*, 2002, **41**, 827-830; f) A. Salomon, R. Arad-Yellin, A. Shanzer, A. Karton and D. Cahen, *J. Am. Chem. Soc.*, 2004, **126**, 11648-11657.
- 8 a) J. M. Seminario, A. G. Zacarias and J. M. Tour, *J. Am. Chem. Soc.*, 2000, **122**, 3015-3020; b) Y. Karzazi, J. Cornil and J. L. Br das, *Nanotechnology*, 2003, **14**, 165-171; c) E. G. Emberly, G. Kirzenow, *Phys. Rev. B*, 2001, **64**, 125318.
- 9 M. Galperin, M. A. Ratner and A. Nitzan, *Nano Lett.*, 2005, **5**, 125-130.
- 10 a) J. Bañuelos, *Chem. Rec.* 2016, **16**, 335-348; b) H. Lu, J. Mack, Y. Yang and Z. Shen, *Chem. Soc. Rev.*, 2014, **43**, 4778-4823.
- 11 a) S. Cherumukkil, B. Vedhanarayanan, G. Das, V. K. Praveen and A. Ajayaghosh, *Bull. Chem. Soc. Jpn*, 2018, **91**, 100-120; b) J. D. Dunitz and R. Taylor, *Chem.-Eur. J.*, 1997, **3**, 89-98; c) T. S. Thakur, M. T. Kirchner, D. Blaser, R. Boese and G. R. Desiraju, *CrystEngComm*, 2010, **12**, 2079-2085; d) E. A. Meyer, R. K. Castellano and F. Diederich, *Angew. Chem., Int. Ed.*, 2003, **42**, 1210-1250.

- 12 a) S. Thakare, P. Stachelek, S. Mula, A. B. More, S. Chattopadhyay, A. K. Ray, N. Sekar, R. Ziessel and A. Harriman, *Chem. Eur. J.*, 2016, **22**, 14356-14366; b) S. Mula, K. Elliott, A. Harriman and R. Ziessel, *J. Phys. Chem. A*, 2010, **114**, 10515-10522.
- 13 A. Bessette and G. S. Hanan, *Chem. Soc. Rev.*, 2014, **43**, 3342-3405.
- 14 D. K. Aswal, S. P. Koiry, B. Jousseme, S. K. Gupta, S. Palacin and J. V. Yakhmi, *Physica E: Low-dimensional Systems and Nanostructures*, 2009, **41**, 325-344.
- 15 R. M. Metzger, J. W. Baldwin, W. J. Shumate, I. R. Peterson, P. Mani, G. J. Mankey, T. Morris, G. Szulczewski, S. Bosi, M. Prato, A. Comito and Y. Rubin, *J. Phys. Chem. B*, 2003, **107**, 1021-1027.
- 16 M. W. Schmidt, K. K. Baldrige, J. A. Boatz, S. T. Elbert, M. S. Gordon, J. H. Jensen, S. Koseki, N. Matsunaga, K. A. Nguyen, S. Su, T. L. Windus, M. Dupuis and J. A. Montgomery Jr, *J. Comput. Chem.*, 1993, **14**, 1347-1363.
- 17 S. Lenfant, C. Krzeminski, C. Delerue, G. Allan and D. Vuillaume, *Nano Lett.*, 2003, **3**, 741-746.

View Article Online  
DOI: 10.1039/C9CP05918K